Universality in the Frenkel-Kontorova model with a cosh-type interaction

Chung-I Chou,[1] Choon-Lin Ho,[1] and Bambi Hu[2,3]
[1]*Department of Physics, Tamkang University, Tamsui, Taiwan 25137, Republic of China*
[2]*Department of Physics and Centre for Nonlinear and Complex Systems, Hong Kong Baptist University, Kowloon, Hong Kong*
[3]*Department of Physics, University of Houston, Houston, Texas 77204-5506*
(Received 16 April 1996; revised manuscript received 6 December 1996)

We have studied a generalized Frenkel-Kontorova model with a cosh-type interaction. A distinctive feature of the model is that the winding number of the last Kolmogorov-Arnold-Moser torus could deviate from the golden mean value for a very large degree of nonlinearity. The singularity spectrum and the generalized fractal dimension depend on the nonlinearity spectrum. However, the critical exponents of the gap in the phonon spectrum, the correlation length, and the Peierls-Nabarro barrier are found to be the same as those found in the standard and Toda Frenkel-Kontorova models. Our conclusions agree with previous findings. [S1063-651X(97)10004-6]

PACS number(s): 05.45.+b, 64.70.Rh, 05.70.Jk

I. INTRODUCTION

The Frenkel-Kontorova (FK) model [1,2] is a simple one-dimensional model used to study incommensurate structures appearing in many condensed-matter systems, such as charge-density waves, magnetic spirals, and adsorbed monolayers [3]. These modulated structures arise as a result of the competition between two or more length scales. The FK model describes a chain of atoms connected by harmonic springs subjected to an external sinusoidal potential. The potential energy of the system is given by

$$H=\sum_i \left[\frac{1}{2}\,(x_{i+1}-x_i-\gamma)^2+\frac{k}{(2\pi)^2}\,(1-\cos 2\pi x_i)\right]. \tag{1}$$

Here x_i is the position of the ith atom, γ the natural length of the spring, and k the rescaled strength of the external potential compared to that of the spring potential. Extensive studies of this model have been made since its introduction. However, in the earlier studies, the FK model was treated in the continuum approximation. Although the continuum approximation, which leads to the sine-Gordon equation and its soliton solutions, provides some quantitative understanding, it is seriously inadequate and misses many essential features. It was not until Aubry [4] reverted to the original discrete version and made use of the Kolmogorov-Arnold-Moser (KAM) theorem that an entirely new approach to the FK model was ushered in. In this approach, the connection between the FK model and the so-called ''standard map'' is especially useful.

Aubry showed that when the mean distance (also called winding number) between successive atoms,

$$\omega=\lim_{n\to\infty}\frac{x_n-x_0}{n}, \tag{2}$$

is rational, the system is always pinned. However, if ω is irrational, there exists a critical k_c such that when $k<k_c$, the system is unpinned; yet when $k>k_c$, the system becomes pinned. This transition, called by Aubry [4] a ''transition by breaking of analyticity,'' is closely connected with the breakup of a KAM torus. It is very analogous to a phase transition, and various critical exponents and questions of universality can be studied. A study of the exponents based on a renormalization theory was carried out by MacKay [5].

On the other hand, multifractal properties and global universality in the FK model had also been studied [6]. The phase diagram of the FK model contains infinitely many tongues of commensurate phases separated by gaps of incommensurate structures. The period of these structures is described by a devil's staircase (DS) function when the parameters defining the model is varied. In [6] it is shown that the devil's staircase constructed along the critical line, which is the collection of critical points k_c for all irrational ω, is a multifractal. Various fractal dimensions were computed in [6].

While interactions in some systems can be approximated by a harmonic potential as described in the standard FK model, there are many physical systems in which the potential is far from harmonic. It is therefore of interest to investigate local and global properties of FK models with nonlinear interactions. In [7] a Toda-type FK model, in which the harmonic potential was replaced by a Toda potential, was considered. It is shown that all the local critical exponents of the Toda FK model are the same as those in the standard FK model. Hence they are in the same universality class. The global properties obtained in [7] cannot be compared with those in [6], since the DS in [7] is constructed at the critical golden mean value $k_c(\omega_G)$, rather than along the critical lines as was the case in [6].

In this paper we study universality properties of a generalized FK model with an anharmonic cosh-type potential. The model is defined by the Hamiltonian [8]

$$H=\sum_i \left\{\sigma^2\left[\cosh\left(\frac{x_{i+1}-x_i-\gamma}{\sigma}\right)-1\right]+\frac{k}{(2\pi)^2}\,(1-\cos 2\pi x_i)\right\}, \tag{3}$$

where σ is a nonlinearity parameter measuring the degree of anharmonicity. When σ tends to infinity, the cosh potential reverts to the harmonic form (standard FK model); as σ de-

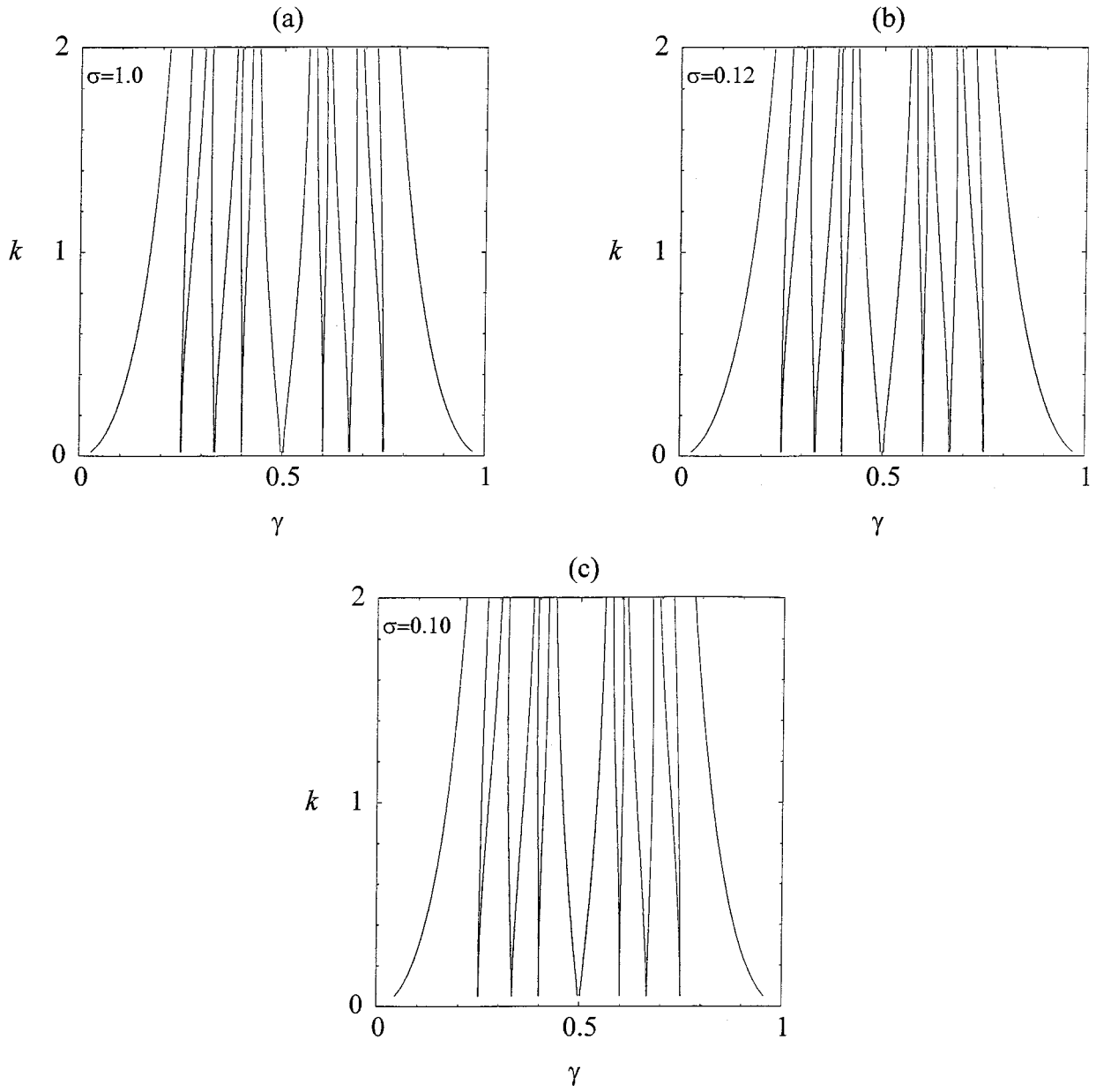

FIG. 1. Phase diagram of the cosh FK model at the fourth Farey generation for $\sigma=1.0$, 0.12, and 0.10.

creases, the potential becomes more and more nonlinear, and in the limit $\sigma\rightarrow 0$, it becomes a δ potential. We will study the phase diagram, the multifractal properties, and the critical behaviors of the cosh FK model, following the procedures in [7]. However, unlike the standard and the Toda FK models, here a complication arises. In Eq. (3), γ appears with the term $(x_{i+1}-x_i)$ in the exponent. This will make the boundaries of the phase diagram an implicit function of γ and the map dependent on γ. In Sec. II, multifractal properties of the model are presented for DS's constructed along the critical line. Critical exponents are presented in Sec. III. Section IV concludes the paper.

II. MULTIFRACTAL STRUCTURES

A. Phase diagram

Following [7], we use both the gradient method [4] and the Newton method [9] to locate the periodic ground states. The phase diagram consists of commensurate and incommensurate ground states in the parameter space of k and γ. For any given rational winding number ω, there is a corresponding commensurate area (Arnold's tongue) in which ω is constant. Between any two tongues there is a gap that contains incommensurate states as well as higher-order commensurate states.

Biham and Mukamel [6] have used the Farey tree construction to study the phase diagram. There are $2^{n-1}+1$ rationals (hence tongues) in the nth Farey generation in the interval [0,1]. The most effective way to construct a phase diagram is to locate the boundaries of commensurate states. For a given commensurate state $\omega=p/q$, its left boundary is determined by equating the energy of that tongue to the energy of an incommensurate state $\overline{\omega}$ in the immediate left neighborhood of the tongue: $H(\beta;\omega,k,\gamma_B)=H(\beta;\overline{\omega},k,\gamma_B)$. Since they have the same k and μ, and $\overline{\omega}$ is infinitely close to ω, their energy should also be infinitely

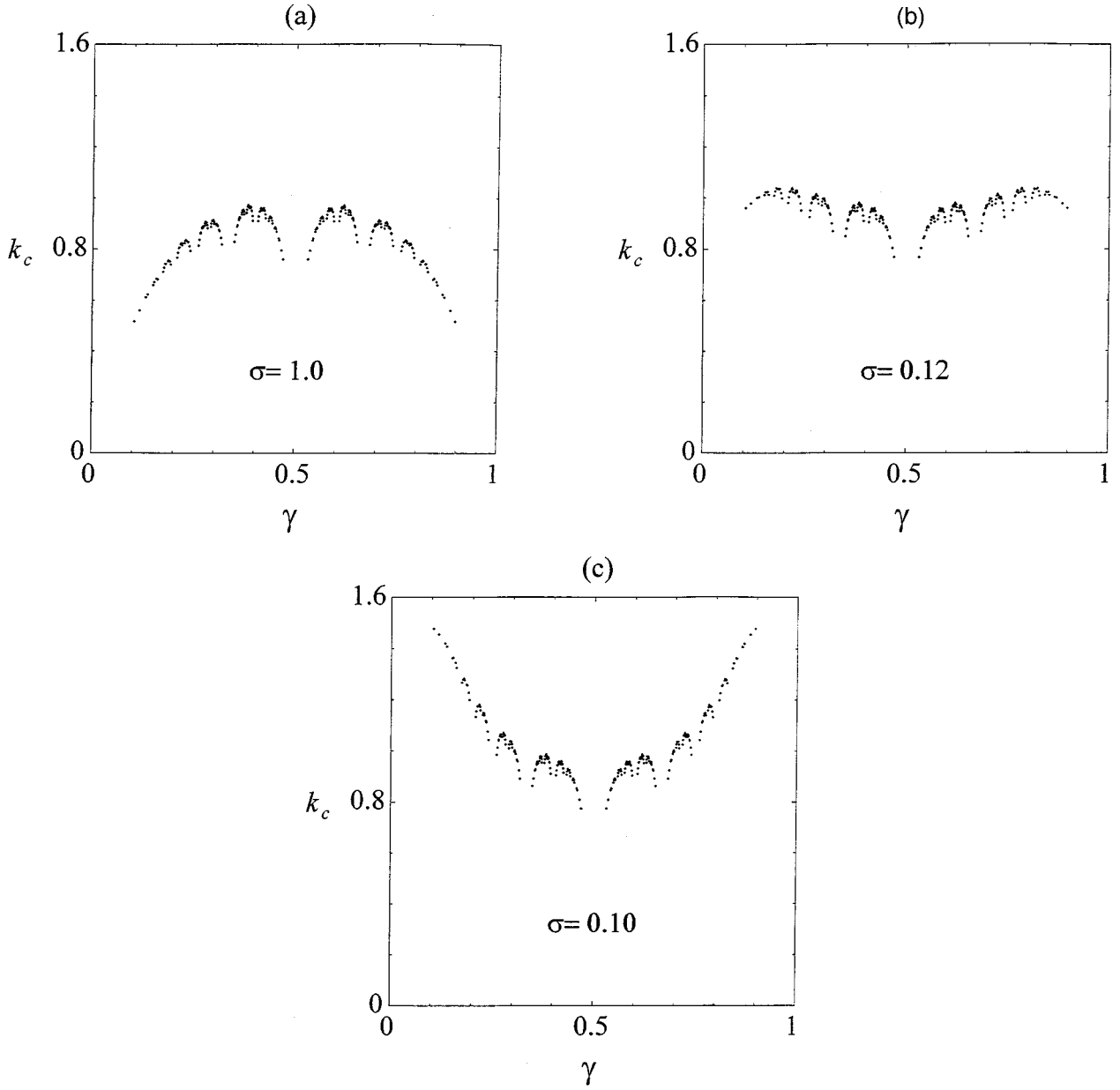

FIG. 2. Critical line of the cosh FK model for $\sigma=1.0$, 0.12, and 0.10.

close. In practical calculations, the incommensurate $\overline{\omega}$ is approximated by a left neighboring tongue $\overline{\omega}=\overline{p/q}$ of a much higher order, i.e., $\overline{q} \gg q$. The higher the order the better the approximation. We found that using $\overline{\omega}$ six orders higher than ω gives very good accuracy. The right boundary is determined in a similar way. As mentioned before, the boundary γ_B cannot be given as an explicit function of β, k, ω, and $\overline{\omega}$, as in the standard and Toda-type FK models [7].

In Fig. 1 we show the phase diagrams at the fourth Farey generation for $\sigma=1.0$, 0.12, and 0.10, respectively. We see that the phase diagrams for the cosh FK model are essentially the same as that for the standard FK model when $\sigma \geqslant 1$. However, for those phase diagrams corresponding to $\sigma \ll 1$, the widths of the gaps between tongues are widened as k increases. In any case, the phase diagrams are symmetric about $\gamma=\frac{1}{2}$, as is the case in the standard FK model.

B. Critical line, devil's staircase, singularity spectrum, and generalized dimension

As already mentioned in the Introduction, if ω is rational, the system is always pinned. But when ω is irrational, there exists a critical k_c such that when $k<k_c$, the system is unpinned; and when $k>k_c$, the system becomes pinned. The collection of critical points k_c for all irrational ω $(0<\omega<1)$ is called the critical line $k_c(\omega)$. It has been shown that on the critical line $k_c(\omega)$, the frequency ratio ω as a function of the parameter γ forms a devil's staircase [6]. This function contains only steps, each of them representing a stable commensurate state. Magnification of any part of the curve (not within a step) will reproduce the original curve.

In order to calculate $k_c(\omega)$, we use both the Greene method [10,11] and the phonon spectrum method [12]. Here the Greene method provides a more accurate determination of k_c for a given ω.

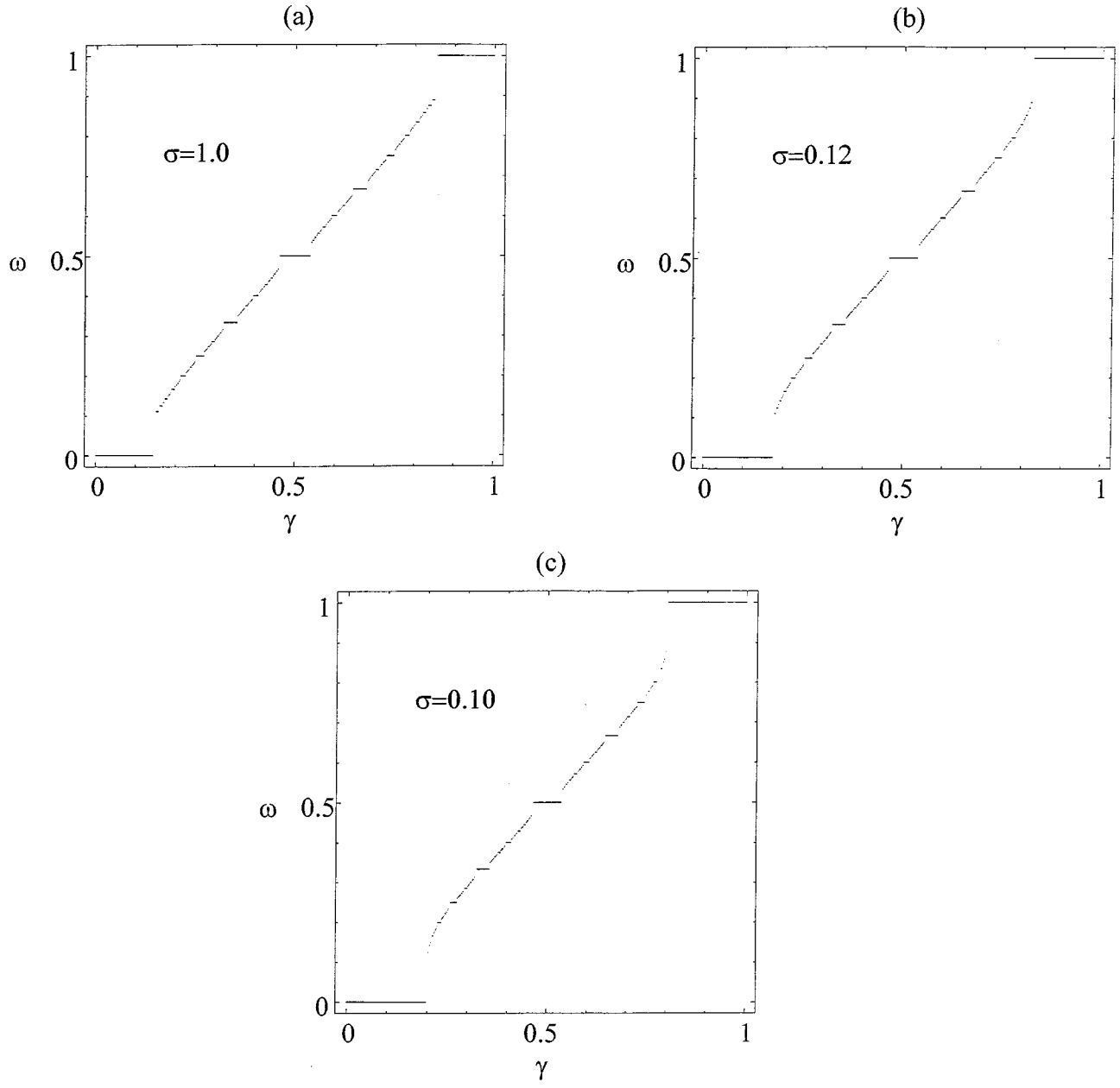

FIG. 3. Devil's staircase of the cosh FK model for $\sigma=1.0$, 0.12, and 0.10. Staircases up to the ninth Farey generation are shown.

Figure 2 presents the critical lines for $\sigma=1.0,0.12,0.10$ and Fig. 3 shows the devil's staircases constructed along these critical lines. We see that the two wings of the critical lines are raised and the lowest and the highest steps in the DS's widen as the nonlinearity of the cosh potential increases (σ becomes smaller).

We can study the multifractal properties of the DS's by defining a fractal measure on the fractal [6,13]. Let us consider a DS constructed up to the nth Farey generation. The corresponding complementary set of this staircase has 2^{n-1} pieces (gaps) in the interval [0,1]. Denote by l_i the width of the ith piece, and m_i the fractal measure defined to be the difference between the winding numbers of two neighboring steps:

$$m_i=\omega_{i+1}-\omega_i, \quad i=1,2,\ldots,2^{n-1}. \tag{4}$$

Thus m_i satisfies the normalization condition

$$\sum_i m_i=1. \tag{5}$$

The partition function $\Gamma^{(n)}(q,\tau)$ of this multifractal in the nth Farey generation is then

$$\Gamma^{(n)}(q,\tau)=\sum_{i=1}^{2^{n-1}} \frac{m_i^q}{l_i^{\tau(q)}}. \tag{6}$$

The function $\tau(q)$ can be obtained by equating (6) to a finite constant C, as were done in [6,7]. However, in order to improve on convergence in our computation, we prefer here

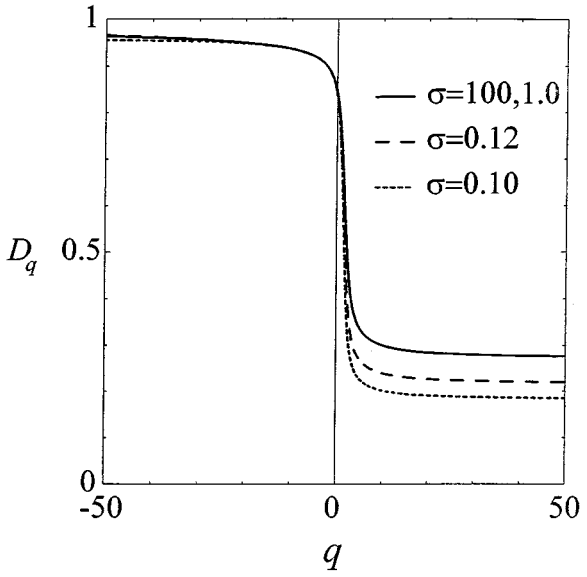

FIG. 4. Generalized dimension D_q of the devil's staircase for $\sigma=100$, 1, 0.12, and 0.10.

to use the ratio trick [13], according to which one considers the ratio of the partition functions in different Farey generations:

$$\frac{\Gamma^{(n+1)}(q,\tau)}{\Gamma^{(n)}(q,\tau)}=1. \tag{7}$$

The convergence increases as n increases. We used $n=9$ in our calculations. Once $\tau(q)$ is obtained, we can compute its derivative $\alpha(q)$

$$\alpha(q)=\frac{d}{dq}\,\tau(q). \tag{8}$$

The singularity spectrum $f(\alpha)$ and the generalized dimension D_q can then be calculated:

$$f(\alpha)=q\alpha(q)-\tau(q), \tag{9}$$

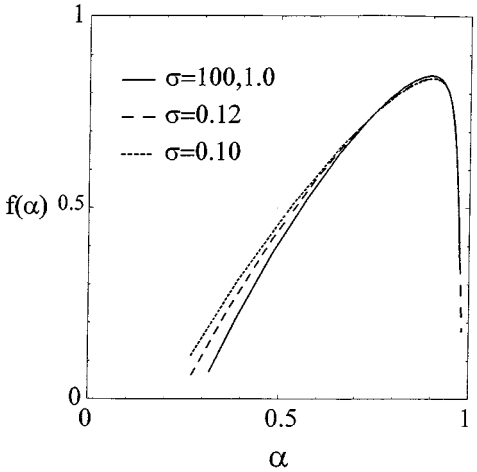

FIG. 5. Singularity spectrum $f(\alpha)$ of the devil's staircase for $\sigma=100$, 1, 0.12, and 0.10.

TABLE I. Winding number ω_{last} of the last KAM torus as a function of the nonlinearity parameter σ and the natural interatomic length γ. The symbol $\langle n\rangle$ denotes the continued fraction $[0,1,n,1,1,1,\ldots]$.

	σ					
γ	1.00	0.80	0.60	0.40	0.20	0.10
0.10	⟨1⟩	⟨1⟩	⟨2⟩	⟨3⟩	⟨5⟩	⟨9⟩
0.20	⟨1⟩	⟨1⟩	⟨2⟩	⟨3⟩	⟨5⟩	⟨9⟩
0.30	⟨1⟩	⟨1⟩	⟨2⟩	⟨2⟩	⟨5⟩	⟨9⟩
0.40	⟨1⟩	⟨1⟩	⟨1⟩	⟨2⟩	⟨5⟩	⟨9⟩
0.50	⟨1⟩	⟨1⟩	⟨1⟩	⟨2⟩	⟨4⟩	⟨9⟩
	$1-\langle1\rangle$	$1-\langle1\rangle$	$1-\langle1\rangle$	$1-\langle2\rangle$	$1-\langle4\rangle$	$1-\langle9\rangle$
0.60	$1-\langle1\rangle$	$1-\langle1\rangle$	$1-\langle1\rangle$	$1-\langle2\rangle$	$1-\langle5\rangle$	$1-\langle9\rangle$
0.70	$1-\langle1\rangle$	$1-\langle1\rangle$	$1-\langle2\rangle$	$1-\langle2\rangle$	$1-\langle5\rangle$	$1-\langle9\rangle$
0.80	$1-\langle1\rangle$	$1-\langle1\rangle$	$1-\langle2\rangle$	$1-\langle3\rangle$	$1-\langle5\rangle$	$1-\langle9\rangle$
0.90	$1-\langle1\rangle$	$1-\langle1\rangle$	$1-\langle2\rangle$	$1-\langle3\rangle$	$1-\langle5\rangle$	$1-\langle9\rangle$

$$D_q=\frac{\tau(q)}{q-1}. \tag{10}$$

We have calculated $f(\alpha)$ and D_q of the devil's staircase for different σ values. The numerical results are shown in Figs. 4 and 5. We find that for $\sigma>1$ the D_q curve coincides, as it should, with the D_q curve in the standard FK model, which we also computed by the same method. For this curve we have the Hausdorff dimension $D_0=0.845\pm0.002$, $D_{50}=0.28\pm0.01$, and $D_{-50}=0.96\pm0.01$. As σ decreases, both D_0 and D_∞ decrease, while $D_{-\infty}$ remains practically unchanged. For instance, for $\sigma=0.10$, we have $D_0=0.836\pm0.002$, $D_{50}=0.21\pm0.01$, and $D_{-50}=0.97\pm0.01$. One may understand this as such. From Fig. 3 we see that as σ decreases, it is the upper and lower steps that widen significantly. These parts correspond to large m_i. From Eq. (6), we see that it is $\tau(q)$ with $q\gg1$ that are affected by these changes. In fact, increases in l_i corresponding to these steps force $\tau(q)$, and hence D_q, to decrease for large q according to Eq. (6). Figure 5 shows the corresponding graphs of the

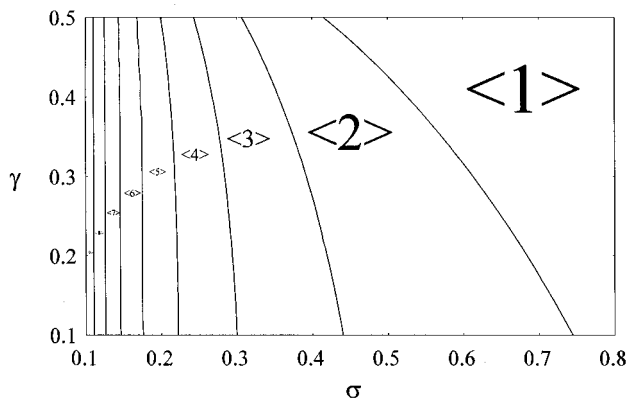

FIG. 6. Winding number ω_{last} as a function of σ and γ for $0.1\leqslant\sigma\leqslant0.8$ and $0.1\leqslant\gamma\leqslant0.5$. The symbol $\langle n\rangle$ denotes the continued fraction $[0,1,n,1,1,\ldots]$. For $0.5\leqslant\gamma\leqslant1$, $\omega_{\text{last}}(\omega,\sigma)=1-\omega_{\text{last}}(1-\gamma,\sigma)$.

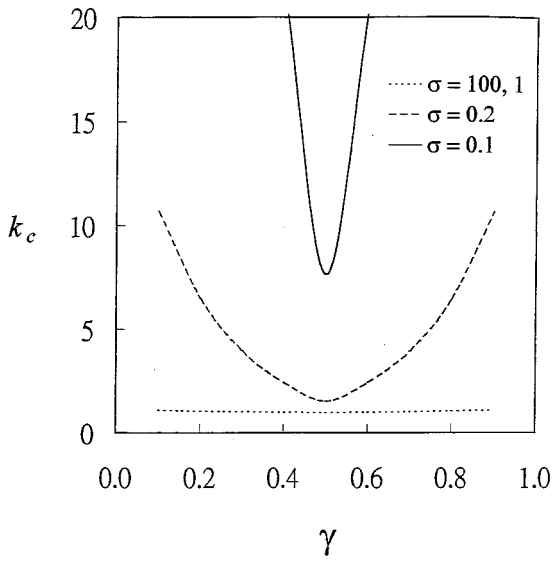

FIG. 7. Critical value $k_c(\omega_{\rm last})$ for the breaking up of the last KAM torus as a function of γ at various values of σ.

singularity spectrum $f(\alpha)$. We see that $f(\alpha)$ increases for $\alpha<0.75$ and slightly decreases for $\alpha>0.75$.

Our results on the D_q and $f(\alpha)$ curves differ from those obtained in [6] (cf. Figs. 8 and 9 in [6]). For instance, the generalized fractal dimensions obtained in [6] are $D_{50}\approx 0.30$, $D_{-50}\approx 1.1$, and $D_0=0.87\pm 0.02$, which is said to be equal within the numerical uncertainty to the Hausdorff dimension of the critical line of the circle map [13]. We believe the discrepancy between our results and those in [6] lies in the empirical formulas introduced in [6] to obtain a sequence of $D_0^{(n)}$ to estimate D_0 (cf. Fig. 5 of [6]).

III. CRITICAL BEHAVIORS

A. Map and critical point

We now discuss local universality in the cosh FK model. The equilibrium condition $\partial H/\partial x_i=0$ with the Hamiltonian (3) is

$$\sigma\left[\sinh\left(\frac{x_{i+1}-x_i-\gamma}{\sigma}\right)-\sinh\left(\frac{x_i-x_{i-1}-\gamma}{\sigma}\right)\right] - \frac{k}{2\pi}\sin 2\pi x_i=0. \tag{11}$$

If we define a conjugate variable $y_i\equiv x_i-x_{i-1}$, then Eq. (11) can be written as a map

$$y_{i+1}=\sigma\,\sinh^{-1}\left[\sinh\left(\frac{y_i-\gamma}{\sigma}\right)+\frac{k}{2\pi\sigma}\sin 2\pi x_i\right]+\gamma,$$

$$x_{i+1}=x_i+y_{i+1}. \tag{12}$$

This map reduces to the standard map as σ becomes large. When k is small, there are KAM curves in the (x,y) phase space. As k increases, these curves break up one by one, and the continuous KAM curves become Cantori. At $k=k_c$ the last rotational KAM curve corresponding to some winding number $\omega_{\rm last}$ breaks up. One notes the presence of γ in this map, in contrast to the standard case. As a result, k_c depends not only on σ, but also on γ. This is closely related to the critical lines studied in Sec. II B. We have studied the dependence of the $\omega_{\rm last}$ and k_c on σ and γ. k_c is determined using the Greene's residue criterion [10,11] for a given $\omega_{\rm last}$.

TABLE II. Critical value $k_c(\omega_{\rm last})$ for the breaking up of the last KAM torus as a function of the nonlinearity parameter σ and the natural interatomic length γ.

	γ		
σ	0.1	0.30	0.50
0.10	420.3172	56.885 00	7.707 843
0.20	10.687 526	3.958 607 3	1.530 696 5
1.00	1.095 213 9	1.015 387 1	0.976 385 35
100	0.971 647 50	0.971 639 74	0.971 635 88
10000	0.971 635 407	0.971 635 407	0.971 635 407

In Table I and Fig. 6 we show the value of the $\omega_{\rm last}$ as a function of γ and σ. We observe that $\omega_{\rm last}$'s are continued fractions of the form $\langle n\rangle\equiv[0,1,n,1,1,1,\ldots]$ $(n=1,2,3,\ldots)$ for $0<\gamma\leqslant 0.5$. For large σ, n is equal to one, and as σ decreases, n increases consecutively. There is a symmetry $\omega_{\rm last}(\gamma,\sigma)=1-\omega_{\rm last}(1-\gamma,\sigma)$. Figure 7 shows plots of $k_c(\omega_{\rm last})$ as function of γ for different σ. Table II gives the values of critical points k_c for some values of σ and γ. We see that for large σ, k_c is independent of σ and γ, and approaches the same value $k_c=0.971\,635\,40\ldots$ as for the standard map. The corresponding $\omega_{\rm last}$ is also the same as that in the standard map, namely, $\omega_{\rm last}=\omega_{\rm G}$ and/or $1-\omega_{\rm G}$, where $\omega_{\rm G}=(\sqrt{5}-1)/2$ is the golden mean number. But when σ becomes small, k_c increases, especially near the two ends $(\gamma=0,1)$. The $\omega_{\rm last}$'s also deviate from the golden mean value. For record purposes, we also show in Fig. 8 plots of $k_c(\omega)$ as a function of the winding number ω at fixed values of γ and σ. We note the symmetry $k_c(\omega,\gamma,\sigma)=k_c(1-\omega,1-\gamma,\sigma)$.

B. Critical exponents

At the critical point $k=k_c$, a ''transition by breaking of analyticity'' occurs. The hull function [4] describing the incommensurate structure undergoes a transition from an analytic function to a nonanalytic function. Many physical quantities [12,14] also undergo a transition at k_c. We will study in our model the critical behaviors of three quantities, namely, the phonon gap, the coherence length, and the Peierls-Nabarro barrier.

1. Phonon gap

First consider the gap in the phonon spectrum Ω_G. Consider a small vibration of the atoms around their equilibrium positions $\{x_i\}$

$$x_i(t)=x_i+\epsilon_i(t). \tag{13}$$

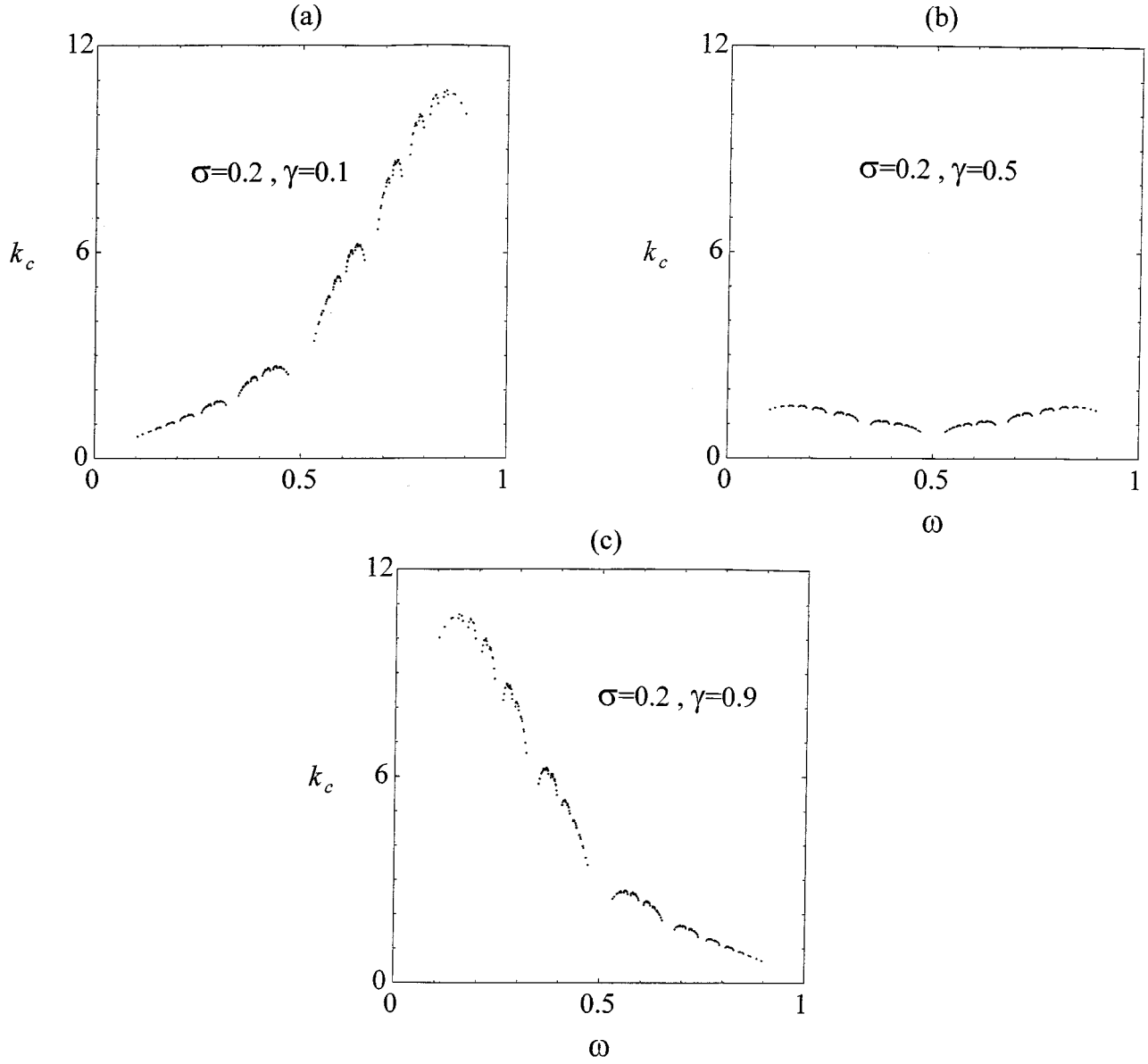

FIG. 8. Critical value $k_c(\omega)$ as a function of winding number of KAM torus at fixed σ and γ.

Then the linearized equation of motion for small vibrations is given by

$$\ddot{\epsilon}_i(t)+\sum_j \frac{\partial^2 H[\{x_i(t)\}]}{\partial x_i(t)\partial x_j(t)}\,\epsilon_j(t)=0, \quad i=1,2,\ldots,q. \tag{14}$$

For the cosh FK model,

$$\frac{\partial^2 H}{\partial x_i \partial x_j}=\begin{cases} -\cosh\left(\dfrac{x_i-x_{i-1}-\gamma}{\sigma}\right), & j=i-1 \\ \cosh\left(\dfrac{x_{i+1}-x_i-\gamma}{\sigma}\right)+\cosh\left(\dfrac{x_i-x_{i-1}-\gamma}{\sigma}\right)+k\,\cos 2\pi x_i, & j=i \\ -\cosh\left(\dfrac{x_{i+1}-x_i-\gamma}{\sigma}\right), & j=i+1. \end{cases} \tag{15}$$

The Fourier transform in time t of Eq. (14) gives

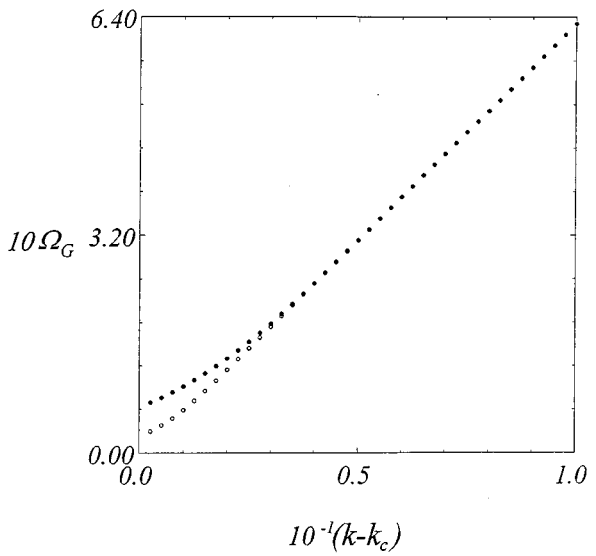

FIG. 9. Gap in the phonon spectrum Ω_{G} as a function of $k-k_c$ for $\sigma=\gamma=0.1$ calculated from two systems with different sizes. The upper one corresponds to $\omega=327/361$ and the lower one to $\omega=856/945$.

$$0=\cosh\left(\frac{x_i-x_{i-1}-\gamma}{\sigma}\right)\epsilon_{i-1}-\left[\cosh\left(\frac{x_i-x_{i-1}-\gamma}{\sigma}\right)+\cosh\left(\frac{x_{i+1}-x_i-\gamma}{\sigma}\right)+k\,\cos 2\pi x_i-\Omega^2\right]\epsilon_i+\cosh\left(\frac{x_{i+1}-x_i-\gamma}{\sigma}\right)\epsilon_{i+1},\quad i=1,2,\ldots,q. \tag{16}$$

The phonon spectrum $\{\Omega_i\}$ is obtained by solving this $q\times q$ matrix equation (16). The gap in the phonon spectrum

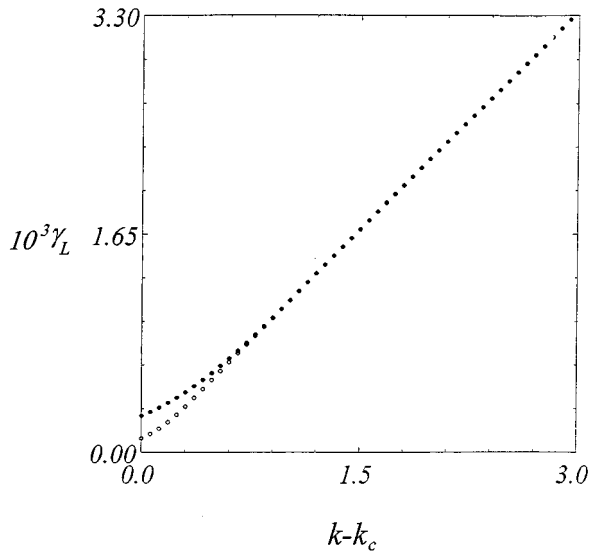

FIG. 10. Lyapunov exponent γ_{L} as a function of $k-k_c$ for $\sigma=\gamma=0.1$. The upper curves corresponds to $\omega=1385/1529$ and the lower one to $\omega=3626/4003$.

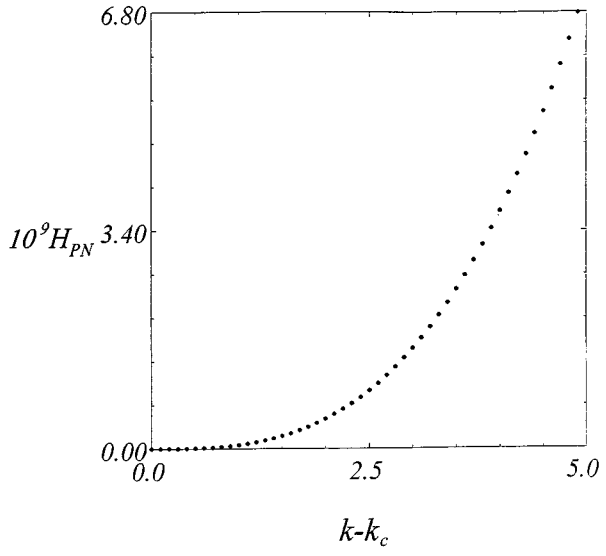

FIG. 11. PN barrier H_{PN} as a function of $k-k_c$ for $\sigma=\gamma=0.1$ calculated for a system with $\omega=3626/4003$.

Ω_{G} is defined to be the lowest phonon frequency in the system, $\Omega_{\mathrm{G}}=\min\{\Omega_i\}$. For $k<k_c$, the ground state of the chain is in a sliding mode and therefore $\Omega_{\mathrm{G}}=0$. As $k>k_c$, a gap Ω_{G} in the phonon spectrum appears and the critical behavior of Ω_{G} can be characterized by the exponent χ [12]

$$\Omega_G(k)\sim(k-k_c)^{\chi}. \tag{17}$$

We have calculated χ for values of σ ranging from 0.1 to 100 and γ from 0.1 to 0.9. Despite the fact that in these ranges of σ and γ, the phase diagram, values of k_c and ω_{last} change greatly, but χ remains unchanged. Our numerical estimate of χ is

$$\chi=1.02\pm0.01. \tag{18}$$

A representative graph of the gap in the phonon spectrum Ω_G as a function of $k-k_c$ is shown in Fig. 9 for $\sigma=\gamma=0.1$.

2. Coherence length

The coherence length ξ measures the distance over which a perturbation δx_i propagates along the chain. An infinitesimal displacement δx_i at x_i will cause a displacement δx_j at x_j, where

$$\delta x_j\sim\exp(-|x_j-x_i|/\xi)\,\delta x_i. \tag{19}$$

Equation (19) defines the correlation length of the ground state. It can be shown [12] that ξ is the inverse of the Lyapunov exponent γ_{L}

$$\xi=\frac{1}{\gamma_{\mathrm{L}}}. \tag{20}$$

One can calculate the Lyapunov exponent from the eigenvalue of the Jacobian matrix of map (12).

In the sliding mode, $k<k_c$, $\xi\to\infty$, since the chain can slide freely under an infinitesimal displacing force. For $k>k_c$, the atoms are locked, ξ is therefore finite and so is γ_{L}. The exponent ν describes the critical behavior of γ_{L}:

$$\gamma_{\mathrm{L}}(k)\sim(k-k_c)^{\nu}. \tag{21}$$

As in the case of χ, the values of ν for various σ and γ we considered are all the same:

$$\nu=0.99\pm0.01. \tag{22}$$

In Fig. 10 we show γ_{L} as a function of $k-k_c$ for $\sigma=\gamma=0.1$.

3. Peierls-Nabarro barrier

The Peierls-Nabarro (PN) barrier of the ground state is defined to be the minimal energy barrier that must be overcome to continuously translate the chain of atoms on the external potential. For $k<k_c$, the PN barrier H_{PN} vanishes, since no extra energy is needed to shift the chain in this sliding mode. For $k>k_c$, the ground state is described by a discontinuous hull function which in the (x,y) phase space is represented by a Cantor set. A minimizing periodic orbit $\{(y_i,x_i)\}_{i=1}^{q}$ can be used to approximate this Cantor set [15]. The PN barrier H_{PN} is the energy difference between the minimizing orbit and its companion minimax orbit

$$H_{\mathrm{PN}}=H_{\max}(\omega)-H_{\min}(\omega), \tag{23}$$

where $H_{\max}(\omega)$ $[H_{\min}(\omega)]$ is the energy of the minimax (minimizing) orbit of winding number ω. The critical behavior of H_{PN} obeys the following power law

$$H_{\mathrm{PN}}\sim(k-k_c)^{\psi}. \tag{24}$$

The critical exponent ψ is found to be

$$\psi=3.00\pm0.02 \tag{25}$$

for all σ and γ values we have calculated.

Since all the critical exponents in the cosh FK model are the same as those in the standard and the Toda FK models, these three models belong to the same universality class in the conventional sense. The critical exponents satisfied the scaling law [12]

$$\psi=2\chi+\nu. \tag{26}$$

Figure 11 gives the PN barrier H_{PN} as a function of $k-k_c$ for $\sigma=\gamma=0.1$.

IV. SUMMARY

In this paper we have investigated a generalized FK model with cosh-type interatomic action. We studied both the multifractal structures and critical behaviors of the model. Unlike the standard and the Toda FK models considered previously in the literature, in this model the natural interatomic length γ, as well as the nonlinearity parameter σ, appears in the map constructed from the equation of equilibrium. As a result, both the critical value k_c and the winding number ω_{last} of the last broken up KAM curve depend not only on σ, but also on γ. We found that when $\sigma\gg1$, this model behaves essentially the same as the standard FK model. As σ decreases well beyond unity, the generalized fractal dimensions D_q and the singularity spectrum $f(\alpha)$ change significantly: D_q decreases appreciably for $q\geqslant0$, while $f(\alpha)$ increases for small α and slightly decreases for large α. A distinctive feature of this model, very much unlike the standard and the Toda models, is that for $\sigma<1$, the KAM curves corresponding to the golden mean winding number ω_{G}, or to $1-\omega_{\mathrm{G}}$, are, in general, not the last ones to break up. Despite this fact, we find that the critical exponents of the gap in the phonon spectrum, the correlation length, and the Peierls-Nabarro barrier at $k_c(\omega_{\mathrm{last}})$ at different values of σ and γ are the same as those found in the standard and the Toda FK models. Hence these three systems belong to the same universality class.

It must, however, be emphasized that these three types of interatomic potentials are all of the *convex* type. When the nonlinearity of the Toda and the cosh potentials increases, the atomic configurations of the models are only *smooth deformations* of the corresponding configurations in the standard FK model. Hence, while the phase diagrams are deformed, there appears no new phase structure in Toda and cosh FK models. Such is not the case for FK models with *nonconvex* potentials, in which more complicated phase diagrams are possible. The universality properties of these nonconvex models require a more detailed study. Also, for nonconvex models, the numerical methods we employed here are not guaranteed to yield a ground-state configuration. One must make use of the method of effective potentials developed by Griffiths and collaborators [16]. We hope to report elsewhere on the results of our investigation of a nonconvex FK model with the Morse-type potential [17].

ACKNOWLEDGMENTS

This work was supported in part by the Republic of China through Grant No. NSC 85-2112-M-032-002 (C.I.C. and C.L.H.) and in part by the Research Grants Council RGC/96-97/10 and Faculty Research Grant FRG/95-96/II-09 and FRG/95-96/II-92 (B.H.).

[1] Y. I. Frenkel and T. Kontorova, Zh. Eksp. Teor. Fiz. **8**, 1340 (1938) [Sov. Phys. JETP **13**, 1 (1938)].
[2] F. C. Frank and J. H. van der Merwe, Proc. R. Soc. London, Ser. A **198**, 205 (1949).
[3] P. Bak, Rep. Prog. Phys. **45**, 587 (1982).
[4] S. Aubry, in *Solitons and Condensed Matter Physics*, edited by A. R. Bishop and T. Schneider (Springer-Verlag, Berlin, 1978); J. Phys. (Paris) **44**, 147 (1983); Physica D **7**, 240 (1983); **8**, 381 (1983).
[5] R. S. MacKay, Physica D **50**, 71 (1991); Ph.D. thesis, Princeton University, 1982 (unpublished).
[6] O. Biham and D. Mukamel, Phys. Rev. A **39**, 5326 (1989).

[7] B. Lin and B. Hu, J. Stat. Phys. **69**, 1047 (1992).
[8] J. E. Byrne and M. D. Miller, Phys. Rev. B **39**, 374 (1989).
[9] H. J. Schellnhuber, H. Urbschat, and A. Block, Phys. Rev. A **33**, 2856 (1986); H. J. Schellnhuber, H. Urbschat, and J. Wilbrink, Z. Phys. B **80**, 305 (1990).
[10] J. M. Greene, J. Math. Phys. **20**, 1183 (1979).
[11] S. J. Shenker and L. P. Kadanoff, J. Stat. Phys. **27**, 631 (1982).
[12] M. Peyrard and S. Aubry, J. Phys. C **16**, 1593 (1983); L. de Seze and S. Aubry, *ibid*. **17**, 389 (1984).
[13] T. C. Halsey, M. H. Jensen, L. P. Kadanoff, I. Procaccia, and B. I. Shraiman, Phys. Rev. A **33**, 1141 (1986).
[14] N. Coppersmith and D. S. Fisher, Phys. Rev. B **28**, 2566 (1983).
[15] H. Johannesson, B. Schaub, and H. Suhl, Phys. Rev. B **37**, 9625 (1988).
[16] R. B. Griffiths and W. Chou, Phys. Rev. Lett. **56**, 1929 (1986); W. Chou and R. B. Griffiths, Phys. Rev. B **34**, 6219 (1986); R. B. Griffiths, in *Fundamental Problems in Statistical Mechanics VII*, edited by H. van Beijeren (North Holland, Amsterdam, 1990), p. 69; K. E. Bassler and R. B. Griffiths, Phys. Rev. B **49**, 904 (1994).
[17] C.-I. Chou, C.-L. Ho, B. Hu, and H. Lee (unpublished).